

UNCLASSIFIED

AD 286 961

*Reproduced
by the*

**ARMED SERVICES TECHNICAL INFORMATION AGENCY
ARLINGTON HALL STATION
ARLINGTON 12, VIRGINIA**



UNCLASSIFIED

NOTICE: When government or other drawings, specifications or other data are used for any purpose other than in connection with a definitely related government procurement operation, the U. S. Government thereby incurs no responsibility, nor any obligation whatsoever; and the fact that the Government may have formulated, furnished, or in any way supplied the said drawings, specifications, or other data is not to be regarded by implication or otherwise as in any manner licensing the holder or any other person or corporation, or conveying any rights or permission to manufacture, use or sell any patented invention that may in any way be related thereto.

63-1-3

NAVWEPS REPORT 7917
NOTS TP 2931
COPY 88

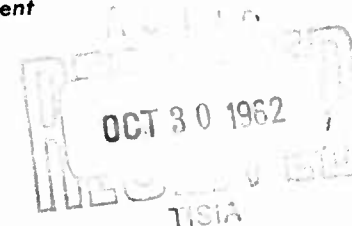
286961

DETECTION AND EVALUATION OF INTERFACE SEPARATIONS IN ROCKET MOTORS

by

J. I. Bujes

Propulsion Development Department



ABSTRACT. Unbonded areas at the interfaces in rocket motors can be detected by radiographs taken tangentially to the critical surfaces. Separations can be reliably determined even when the radial dimension is as small as 0.001 inch. The procedure offers a method for in-process and end-product inspection.

Released to ASTIA for further dissemination with
out limitations beyond those imposed by security
regulations.

286 961



U. S. NAVAL ORDNANCE TEST STATION

China Lake, California

August 1962

U. S. NAVAL ORDNANCE TEST STATION

AN ACTIVITY OF THE BUREAU OF NAVAL WEAPONS

C. BLENMAN, JR., CAPT., USN WM. B. MCLEAN, PH.D.
Commander Technical Director

FOREWORD

Uniform burning of propellant is a major factor in the performance of rocket motors with solid propellant grains. Interface separations between adjacent materials - casing, liner, thermal insulator, propellant grain - may permit undesired ignition and irregular combustion. Function of the rocket motor may be impaired even to the point of failure. Hence the determination of the existence and especially the dimensions of such separations is of great importance.

This report presents the theoretical considerations for the determination of interface separations by radiography and the experimental verification of these considerations. The theoretical considerations and the experimental data apply to the POLARIS Missile. The findings, however, are applicable to all solid propellant rocket motors of comparable size.

The great value of this work has been recognized in the form of a Navy Superior Civilian Service Award to the Author, Dr. J. I. Bujes. In making the award Admiral W. F. Raborn said "This system is now in full-scale operation is developing into a key item in the Production Acceptance Tests of POLARIS motors.....and is currently being prepared as an Ordnance Specification." Perhaps of even greater satisfaction to the Author has been the conspicuous success in forecasting the behavior of POLARIS motors.

This work was accomplished under Task Assignment SP71402-5.

F. MC CULLOUGH, JR.
Head, Test and Evaluation
Division

Released under
the authority of:

JAMES T. BARTLING

Head, Propulsion Development
Department

NOTS Technical Publication 2931
NAVWEPS REPORT 7917

Published by Propulsion Development Department
Collation Cover, 8 leaves, abstract cards
First printing 270 numbered copies
Security classification UNCLASSIFIED

- 2 Office of the Deputy Commander AFSC for Aerospace Systems, Los Angeles
Dr. P.K. Leatherman (BSREQ) (1)
Major Harned (1)
- 1 Tactical Air Command, Langley Air Force Base (TPL-RQD-M)
- 6 Aerojet-General Corporation, Sacramento, via BuWepsRRRep
Department 3770 (2)
Department 5270 (2)
Department 6600 (2)
- 1 Aerojet-General Neucleonics, San Ramon, Calif. (P. E. Underhill)
- 3 Allegany Ballistics Laboratory, Cumberland, Md.
E. D. Harvey (1)
Ron Downey (1)
R. J. Mascis (1)
- 1 Bruce H. Sage, Consultant, Pasadena
- 2 Hercules Powder Company, Magna, Utah
R. L. Durand (1)
Sanford Gross (1)
- 1 Jet Propulsion Laboratory, CIT Pasadena (G. W. Lewis)
- 3 Lockheed Aircraft Corporation, Missiles and Space Division, Palo Alto, Calif.
LMSC 81-51 (1)
LMSC 81-72 (2)
- 2 Lockheed Aircraft Company Resident Representative, Aerojet-General Corporation, Sacramento, via BuWepsRRRep
- 1 Los Alamos Scientific Laboratory, N. Mex. (Dr. G. H. Tenney)
- 1 Solid Propellant Information Agency, Applied Physics Laboratory, JHU, Silver Spring
- 1 Space Technology Laboratories, Inc., Redondo Beach, Calif.
(Harry Taylor)
- 1 The Boeing Company, Seattle (James M. Baker)
- 2 The Martin Company, Orlando
MP 163, M. G. Miller (1)
MP 348, George J. Marks (1)
- 1 Thiokol Chemical Corporation, Longhorn Ordnance Works, Marshall, Texas (H. L. Bowman)
- 1 Thiokol Chemical Corporation, Redstone Division, Redstone Arsenal (W. W. Mills)
- 2 Thiokol Chemical Corporation, Utah Division, Brigham City
D. W. Rathmann (1)
M. Rubin (1)
- 2 Thiokol Chemical Corporation, Wasatch Division, Tremonton, Utah
D. Liddell (1)
E. C. Goforth (1)
- 1 Thompson Ramo Wooldridge Inc., RW Division, Canoga Park, Calif. (Technical Information Services)
- 148 Joint Army-Navy-Air Force Mailing List for the Distribution of Solid Propellant Technical Information, dated June 1961

CONTENTS

Introduction	1
Theoretical	1
Experimental	8
Conclusions	9
Recommendations	10

Figures

1. Geometry of a Rocket Motor	2
2. Geometry of Separation Depth and Chord Length	2
3. Average Chord Length	3
4. Illustration for X-ray Absorption Calculation	4
5. Film Density Differentials vs. Gap Dimensions	11
6. Film Density Curves With Background	12

INTRODUCTION

Uniform burning of propellant is a major factor in the successful performance of rocket motors with solid propellant grains. The construction of a motor - case, liner, and/or inhibitor, propellant grain - is designed to provide optimum conditions for uniform combustion.

In some cases where the grain must be bonded to the casing, the liner may serve both as inhibitor and bonding agent. Failure of the bonding - regardless of cause - may seriously affect the performance of the motor, even to complete failure. The most critical area of separation is the interface between the propellant grain and the liner.

A reliable method not only for the detection, but also for the determination of the degree of separation, is thus essential, in order to coordinate the dimensions of the separations with rocket performance and so lead to knowledge of acceptable limitations.

The use of x-ray is the method of choice. However, two problems are involved. The first of these is that of obtaining radiographs that can be interpreted with a high degree of uniformity among different observers. The second is to eliminate, as far as possible, the human equation in the evaluation.

THEORETICAL

Consideration of the geometry (Fig. 1) of a rocket motor and of the characteristic x-ray absorption factors of the various materials, forces the conclusion that radiography must be in the direction tangential to the critical area. If the attempt is made to x-ray in a radial direction, a separation of 0.001 inch would not produce a film density differential that could be reliably interpreted.

However, if the x-ray beam passes tangentially through an unbonded area, it is the chord that is traversed. Even with a radial separation distance of only 0.001 inch and a grain diameter of 16.5 inches, the average chord dimension for the area is 0.193 inch. This distance is sufficient to produce film density differences that can be reliably interpreted.

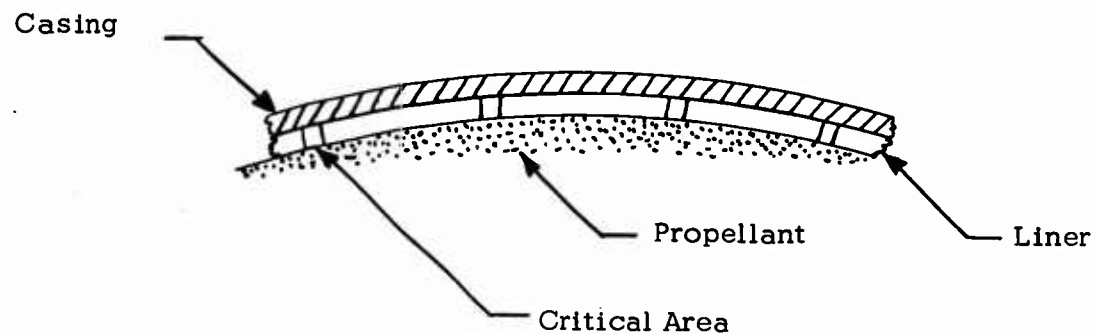
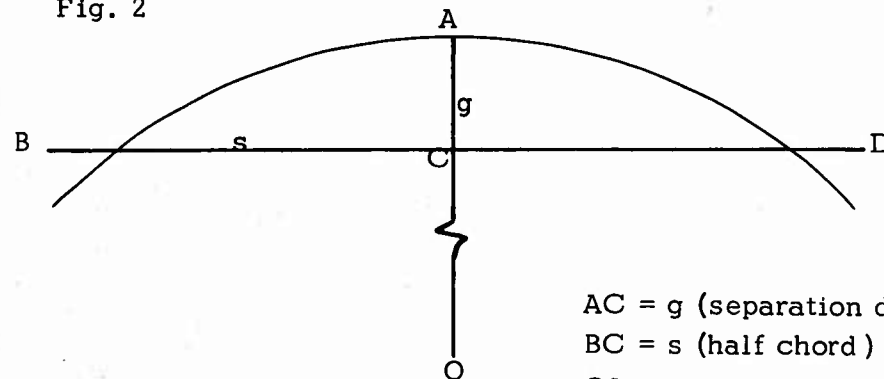


Fig. 1

The geometry of a separation showing the relation between radial separation distance and chord dimension is shown in Figs. 2 and 3. Average chord lengths for grain diameters of 53.5 inches and 16.5 inches are shown in Tables 1 and 4.

Fig. 2



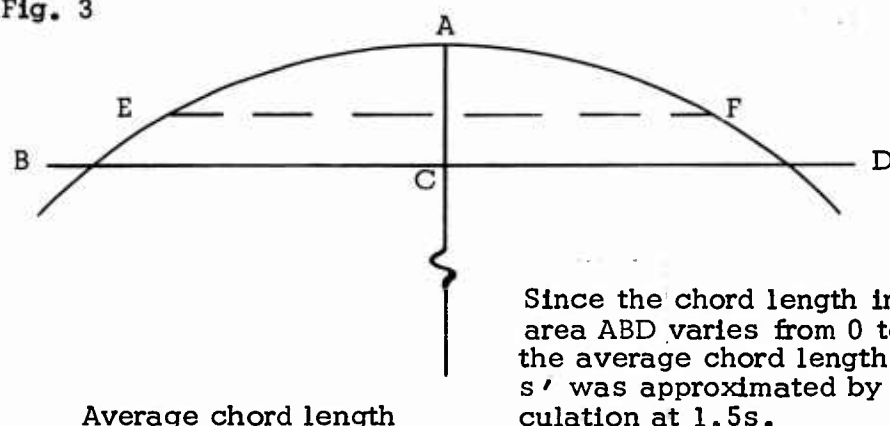
Geometry of separation
depth and chord length

$$\begin{aligned} AC &= g \text{ (separation depth)} \\ BC &= s \text{ (half chord)} \\ OA &= r \\ \text{then } s^2 &= g(2r-g) \\ s &= g \sqrt{2r-g} \end{aligned} \quad (1)$$

Since gaps greater than 0.1 inch radial dimension were not considered, equation (1) can be approximated as

$$s = \sqrt{2gr} \quad (2)$$

Fig. 3



The chord lengths for the air gap and the adjacent material are equal, and the film density difference, ΔD , can be computed from Lambert's basic absorption equation

$$\begin{aligned}
 I_1 &= I_0 e^{-\mu t_1} \\
 I_2 &= I_0 e^{-\mu t_2} \\
 \frac{I_1}{I_2} &= e^{-\mu(t_1 - t_2)} = e^{-\mu(\Delta t)} \quad (3)
 \end{aligned}$$

in which μ is the absorption coefficient and t is the linear dimension of the x-ray path (Fig. 4).

In logarithmic form this becomes

$$\text{Log } I_1 - \text{Log } I_2 = -\mu \Delta t \text{ Log } e.$$

Since $\text{Log}_{10} e = 0.434$, 1 inch = 2.5cm, $s' = \Delta t$, the above may be written

$$\text{Logrelexp}_1 - \text{Logrelexp}_2 = -1.1\mu s'. \quad (4)$$

This must be converted to x-ray absorption coefficient μ_x specific for the energy source and the substances involved.

For Cobalt 60 and propellant ρ 1.7, μ_x is approximately 0.1 and $\Delta \text{Logrelexp} = -.11s'$. For liner ρ 1.05 μ_x is 0.062 and $\Delta \text{Logrelexp} = -.068s'$.

Fig. 4

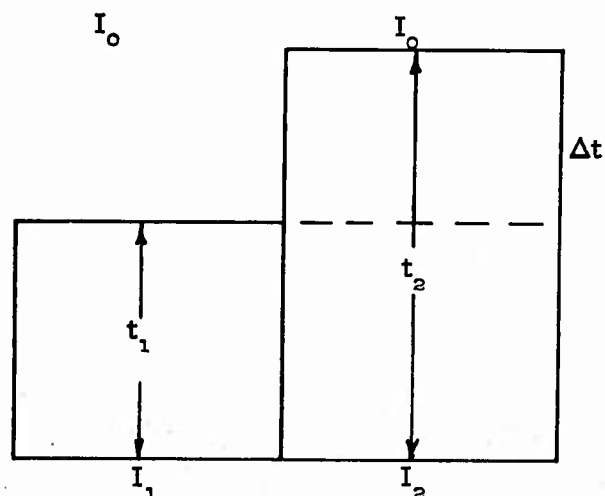


TABLE 1. Radial Interface Separation and Chord Length

g	$g \times 2r$	s	s'
0.001 in.	0.0535 in.	0.232 in.	0.348 in.
.005	.2675	.519	.778
.010	.5350	.733	1.100
.015	.8025	.898	1.347
.020	1.0700	1.038	1.557
.050	2.6750	1.635	2.455
0.100	5.3500	2.320	3.480

$$2r = 53.5 \text{ inches}$$

$$s' = 1.5s$$

In the following tables it is considered that the separation lies between liner and propellant grain, and the film density differentials have been calculated accordingly. Radial dimension of separation is represented by g . The average chord length, s' , is $1.5s$. In all the tables a film density of 3 for the air gap has been assumed. Except in Table 9 the calculations are based upon Cobalt 60 as a source.

TABLE 2. Calculated Film Density Differentials
- Propellant Grain and Air Gap -

g	s'	$\Delta \text{Logrelexp}$	D_1	D_2	ΔD
0.001 in.	0.348 in.	0.0383	3	2.80	0.20
.005	0.778	.0855	3	2.56	.44
.010	1.100	.1210	3	2.40	.60
.015	1.347	.1482	3	2.29	.71
.020	1.557	.1713	3	2.20	.80
.050	2.455	.2700	3	1.86	1.14
0.100	3.480	0.3830	3	1.56	1.44

2r = 53.5 inches

Kodak Film KK

In this table, as in Tables 3, 5, 6, 7 and 8, D_1 , the film density of the air gap, is assumed as 3. D_2 , the film density for the propellant, is calculated thus:

Logrelexp_2 (corresponding to D_3) is diminished by $\Delta \text{Logrelexp}$ to Logrelexp_1 . This makes it possible to derive D_2 from the characteristic x-ray film curve (Fig. 5).

From the x-ray absorption coefficients and the average chord length it is then possible to calculate the film density differentials for the various radial dimensions of unbonded areas. Tables 1 through 9 give these data.

TABLE 3. Calculated Film Density Differentials, ΔD ,
for Liner and Air Gap

g	s'	$\Delta \text{Logrelexp}$	D_1	D_2	ΔD
0.001 in.	0.348 in.	0.0237	3	2.88	0.12
.005	.778	.0530	3	2.72	.28
.010	1.100	.0746	3	2.62	.38
.015	1.347	.0915	3	2.54	.46
.020	1.557	.1060	3	2.47	.53
.050	2.455	.1670	3	2.16	.84
0.100	3.480	0.2370	3	1.81	1.19

2r = 53.5 inches

Kodak Film KK

TABLE 4. Radial Interface Separation and Chord Length

g	g x 2r	s	s'
0.001 in.	0.0165 in.	0.129 in.	0.193 in.
.005	.0825	.289	.434
.010	.1650	.405	.608
.015	.2480	.500	.750
.020	.3300	.577	.865
.050	.8250	.913	1.370
0.100	1.6500	1.650	1.935

2r = 16.5 inches

s' = 1.5 s

TABLE 5. Calculated Film Density Differentials ΔD for Propellant Grain and Air Gap

g	s'	$\Delta \text{Logrelexp}$	D ₁	D ₂	ΔD
0.001 in.	0.193 in.	0.0212	3	2.90	0.10
.005	.434	.0478	3	2.76	.24
.010	.608	.0670	3	2.66	.34
.015	.750	.0825	3	2.59	.41
.020	.865	.0950	3	2.52	.48
.050	1.370	.1510	3	2.24	.76
0.100	1.935	0.2130	3	1.93	1.07

2r = 16.5 inches

Kodak Film KK

TABLE 6. Calculated Film Density Differential ΔD for Liner and Air Gap

g	s'	$\Delta \text{Logrelexp}$	D ₁	D ₂	ΔD
0.001 in.	0.193 in.	0.0131	3	2.935	0.065
.005	.434	.0298	3	2.850	.150
.010	.608	.0415	3	2.790	.210
.015	.750	.0513	3	2.750	.250
.020	.865	.0590	3	2.700	.300
.050	1.370	.0933	3	2.530	.470
0.100	1.935	0.1320	3	2.340	0.660

2r = 16.5 inches

Kodak Film KK

Although the chord length at the smaller radius ($2r = 16.5$ inches) is much less (e.g. at separation depth, - 0.001 inches - 0.193 inches vs. 0.348 inches for $2r = 53.5$ inches), and hence the film density differentials are smaller, even at this separation depth, the film density differential is still 0.065 between air gap and liner.

Two similar computations were made for Kodak Film AA.

TABLE 7. Calculated Film Density Differentials ΔD for Propellant and Air Gap

g	s'	$\Delta \text{Logrelexp}$	D_1	D_2	ΔD
0.001 in.	0.193 in.	0.0212	3	2.87	0.13
.005	.434	.0478	3	2.71	.29
.010	.608	.0670	3	2.64	.36
.015	.750	.0825	3	2.51	.49
.020	.865	.0950	3	2.43	.57
.050	1.370	.1510	3	2.09	.91
0.100	1.935	0.2130	3	1.72	1.28

$2r = 16.5$ inches

Kodak Film AA

TABLE 8. Calculated Film Density Differentials ΔD for Liner and Air Gap

g	s'	$\Delta \text{Logrelexp}$	D_1	D_2	ΔD
0.001 in.	0.193 in.	0.0131	3	2.922	0.078
.005	.434	.0298	3	2.820	.180
.010	.608	.0415	3	2.750	.250
.015	.750	.0513	3	2.690	.310
.020	.865	.0590	3	2.650	.350
.050	1.370	.0933	3	2.450	.550
0.100	1.935	0.1313	3	2.220	0.780

$2r = 16.5$ inches

Kodak Film AA

TABLE 9. Calculated Film Density Differentials ΔD
for Propellant and Air Gap, Using
22 Mev Betatron

g	s'	$\Delta \text{Logrelexp}$	D_1	D_2	ΔD
0.001 in.	0.193 in.	0.008	3	2.952	.048
.005	.434	.018	3	2.892	.108
.010	.608	.025	3	2.850	.150
.015	.750	.031	3	2.814	.186
.020	.865	.035	3	2.790	.210
.050	1.370	.056	3	2.664	.336
0.100	1.935	0.079	3	2.526	.474

$2r = 16.5$ inches

Kodak Film AA

The calculated values for ΔD in Tables 5, 6, 7 and 8 vs. separation depth g are shown in a semi-logarithmic coordinate system in Fig. 5. The close agreement between the two types of film is explained by the assumption of $D = 3$ for the air gap, resulting in maximum contrast, 6 for Film AA and 5 for Film KK.

The preceding computations are based upon radiographs without scattering ⁽¹⁾ or prefogging. An original density curve and the corrections made necessary by increased background due to scattering are illustrated in Fig. 6. It will be noted that the loss of contrast is greatest at low densities and becomes nominal at density 3.

EXPERIMENTAL

According to the theoretical calculations it seemed very highly probable that actual radiography would successfully identify interface separations of very small gap depth.

Accordingly, models were set up in which the air gap between propellant and liner material could be fixed at any desired distance. The outside diameter of the simulated rocket motor cross-section was 24 inches; the steel casing was 0.125 inch in thickness; the rubber insulator material was 0.25 inch. The propellant cross-section diameter was thus 23.25 inches. The air gaps were obtained by the use of shims of the desired dimensions inserted between liner and propellant.

⁽¹⁾ Seeman, H. E., "Secondary Radiation in the Radiography of Aluminum, Steel, and Lead", Communication No. 689, The Eastman Kodak Co.

The x-ray source was a 22 Mev Betatron, with a focal spot one-quarter millimeter square. The distance from source to film was 6 feet, while that from the model to the film was 10 inches.

The theoretical computation of the film density differentials for the Betatron is found in Table 9. The x-ray absorption coefficient for the propellant using the 22 Mev Betatron is 0.037 as compared to 0.1 for the radiation of a Cobalt 60 source.

It is noteworthy that even under these unfavorable conditions air separations as small as 0.001 inch were apparent to the unaided eye. The film density differentials of the critical areas are readily read by the densitometer which gives readings reproducible to ± 0.02 . The trained eye can conservatively distinguish film density differentials of the same order of magnitude.

One of the experiments is illustrated in Fig. 7. In this experiment ρ for the propellant was 1.6, and that of the liner 1.4. The radial dimension of the air gap was 0.003 inch.

It must be noted that this is a positive reproduction of an x-ray film and appears much like an ordinary photograph, in that the air gap is light and the shim areas dark. It is also noticeable (and noteworthy) that the air gap appears in the film to be considerably wider than is actually the case. This phenomenon is the result of several parameters, and is very useful as it makes visual detection of separation areas much easier. Otherwise this apparent difference in dimension is not important as it is only the film density differential that is significant.

CONCLUSIONS

Computations based upon the geometry of a rocket motor and the x-ray absorption coefficients of the materials indicated the feasibility of detecting interface separations in rocket motors even when the radial dimension of the unbonded area is as small as 0.001 inch. These conclusions were amply verified by experiments. Tangential radiography of interface areas in rocket motors thus provides a basis upon which to develop an in-process and end-product inspection.

RECOMMENDATIONS

The suggested method, using a high-energy source such as a 22 Mev Betatron should be developed into a practical inspection method. Exposure times are not excessive for space motors of the dimensions now in use.

However, such a method is already threatened with obsolescence by the demand for solid propellant motors of larger size. Significantly increased dimensions will require intolerably long radiographic exposure times. Further, larger motors will require more radiographs to examine the whole circumference of critical areas. A radiograph covering 15 degrees of circumference may be neither practical nor reliable.

It is therefore strongly urged that other methods of inspection be investigated. The use of scintillators and ancillary equipment might offer a completely filmless process and make possible a completely automated inspection procedure for even the largest space motors.

(1) Seeman, H. E., "Secondary Radiation in the Radiography of Aluminum, Steel, and Lead", Communication No. 689, The Eastman Kodak Company.

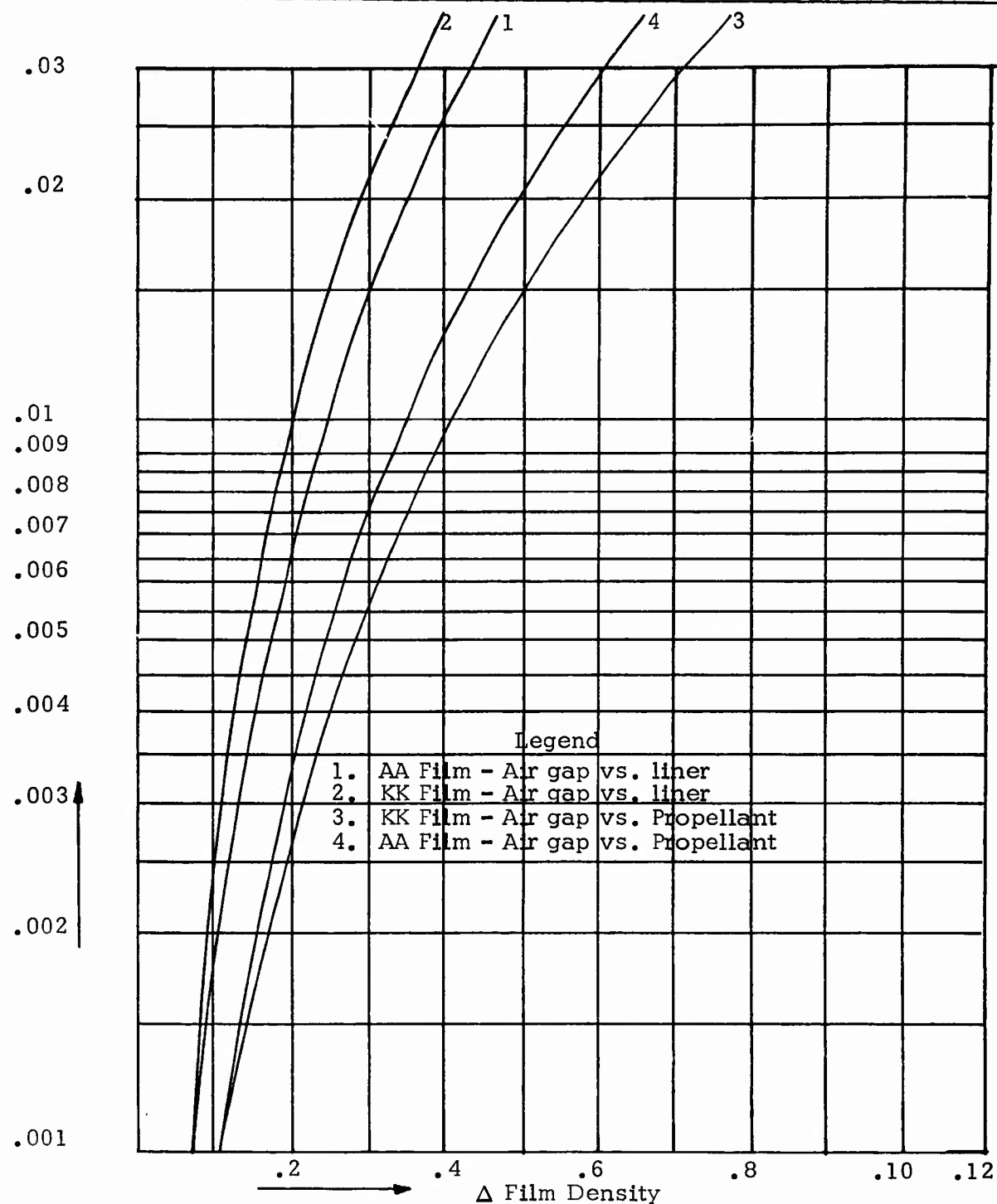


Fig. 5 Film Density Differentials vs. Gap Dimensions

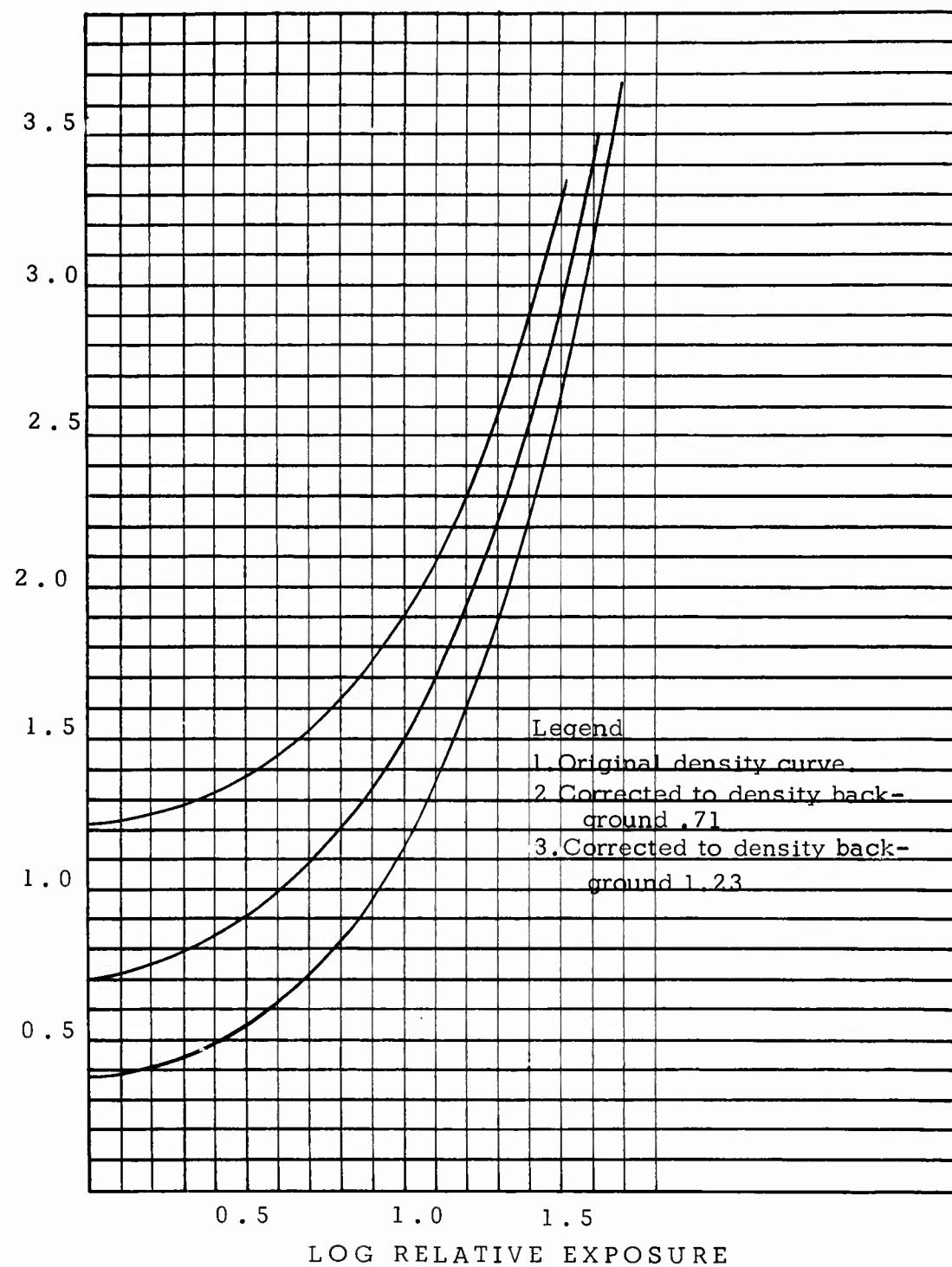


Fig. 6 Density Curves with Background

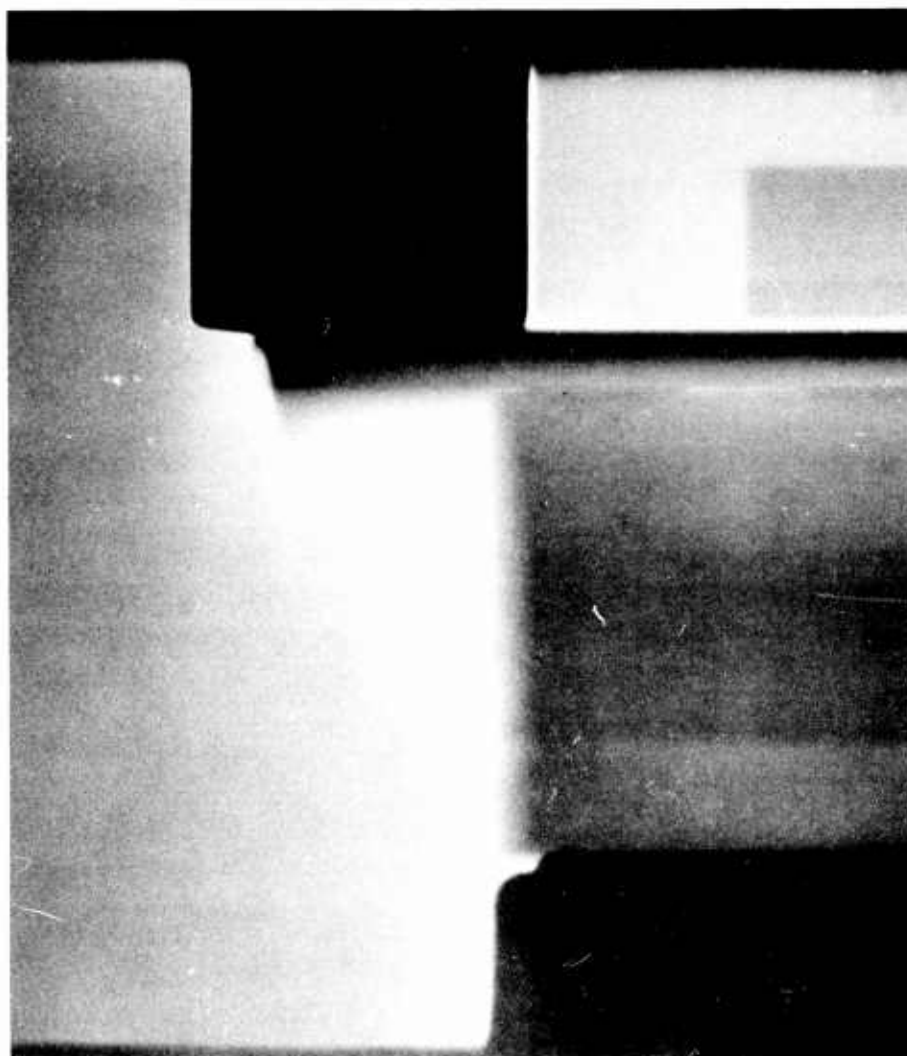


Fig. 7 X-ray of Simulated Motor Section

INITIAL DISTRIBUTION

- 1 Chief, Bureau of Naval Weapons (FWEW)
- 2 Special Projects Office
 - SP 27131 (1)
 - SP 274 (1)
- 4 Chief of Naval Operations (Operations Evaluation Group)
- 1 Chief of Naval Research (Code 104)
- 1 Fleet Anti-Air Warfare Training Center, San Diego (Guided Missile Section)
- 1 Naval Air Material Center, Philadelphia
- 2 Naval Air Mobile Training, Naval Air Station Miramar
 - Naval Air Mobile Training Detachment, 4003 Ordnance (1)
 - Naval Air Mobile Training Detachment, 4030 Missile (1)
- 1 Naval Air Test Center, Patuxent River (Aeronautical Publications Library)
- 1 Naval Ammunition Depot, Concord (QEL - F. C. Hund)
- 1 Naval Avionics Facility, Indianapolis (Library)
- 1 Naval Explosive Ordnance Disposal Technical Center, Naval Propellant Plant, Indian Head
- 1 Naval Ordnance Laboratory, White Oak (E. L. Criscuolo)
- 3 Naval Propellant Plant, Indian Head
 - H. B. Alexander (1)
 - J. E. Wilson (1)
- 1 Naval Radiological Defense Laboratory, San Francisco (Code 942)
- 2 Naval Research Laboratory
 - Code 6210 (1)
 - Code 6254 (1)
- 2 Naval Underwater Ordnance Station, Newport
- 1 Naval Weapons Evaluation Facility, Kirtland Air Force Base (Code 401)
- 2 Naval Weapons Services Office, Naval Weapons Plant
- 1 Operational Test and Evaluation Force
- 1 Bureau of Naval Weapons Branch Representative, Cumberland
- 1 Bureau of Naval Weapons Representative, Azusa, Calif.
- 1 Bureau of Naval Weapons Resident Representative, Sacramento
- 1 Bureau of Naval Weapons Representative, Sunnyvale (SPL 40)
- 1 Army Ballistic Missile Agency, Redstone Arsenal (T.N.L. Pughe ORDAB-RPS)
- 1 Air Force Cambridge Research Laboratories, Laurence G. Hanscom Field
- 2 Air Proving Ground Center, Eglin Air Force Base
 - PGAPI (1)
- 1 Air University Library, Maxwell Air Force Base
- 1 Hill Air Force Base, Ogden (Alex Peresich)

ABSTRACT CARD

<p>U. S. Naval Ordnance Test Station <u>Detection and Evaluation of Interface Separations in Rocket Motors</u>, by J. I. Bujes, China Lake, Calif., NOTS, June 1962. 14 pp. (NAVWEPS Report 7917, NOTS TP 2931), UNCLASSIFIED.</p> <p>ABSTRACT. Unbonded areas at the interfaces in rocket motors can be detected by radiographs taken tangentially to the critical surfaces. Separations can be reliably determined even when the radial dimension is as small as 0.0001 inch. The procedure offers a method for in-process and end-product inspection.</p> <p>○ 1 card, 4 copies</p>	<p>U. S. Naval Ordnance Test Station <u>Detection and Evaluation of Interface Separations in Rocket Motors</u>, by J. I. Bujes, China Lake, Calif., NOTS, June 1962. 14 pp. (NAVWEPS Report 7917, NOTS TP 2931), UNCLASSIFIED.</p> <p>ABSTRACT. Unbonded areas at the interfaces in rocket motors can be detected by radiographs taken tangentially to the critical surfaces. Separations can be reliably determined even when the radial dimension is as small as 0.001 inch. The procedure offers a method for in-process and end-product inspection.</p> <p>○ 1 card, 4 copies</p>
<p>U. S. Naval Ordnance Test Station <u>Detection and Evaluation of Interface Separations in Rocket Motors</u>, by J. I. Bujes, China Lake, Calif., NOTS, June 1962. 14 pp. (NAVWEPS Report 7917, NOTS TP 2931), UNCLASSIFIED.</p> <p>ABSTRACT. Unbonded areas at the interfaces in rocket motors can be detected by radiographs taken tangentially to the critical surfaces. Separations can be reliably determined even when the radial dimension is as small as 0.001 inch. The procedure offers a method for in-process and end-product inspection.</p> <p>○ 1 card, 4 copies</p>	<p>U. S. Naval Ordnance Test Station <u>Detection and Evaluation of Interface Separations in Rocket Motors</u>, by J. I. Bujes, China Lake, Calif., NOTS, June 1962. 14 pp. (NAVWEPS Report 7917, NOTS TP 2931), UNCLASSIFIED.</p> <p>ABSTRACT. Unbonded areas at the interfaces in rocket motors can be detected by radiographs taken tangentially to the critical surfaces. Separations can be reliably determined even when the radial dimension is as small as 0.001 inch. The procedure offers a method for in-process and end-product inspection.</p> <p>○ 1 card, 4 copies</p>